FACTA UNIVERSITATIS
Series: **Physics, Chemistry and Technology** Vol. 13, N^o 3, 2015, pp. 153 - 162
DOI: 10.2298/FUPCT1503153S

TWO-DIMENSIONAL FLUID MODELING OF DC GLOW DISCHARGE IN ARGON AT LOW PRESSURE[†]

UDC 535.52 : 535.56 : 546.293

M. N. Stankov[*], A. P. Jovanović, V. Lj. Marković, S. N. Stamenković

Department of Physics, Faculty of Sciences and Mathematics, University of Niš, Serbia

Abstract. *The modeling of DC glow discharge in argon at the pressure p = 1.5 Torr and inter-electrode distance d = 1 cm was performed for different voltages and glow currents. For the first time, argon glow discharge is modeled using a two-dimensional (2D) fluid model with non-local ionization. A detailed numerical procedure for 2D fluid modeling is given. The 2D profiles of particle number densities and electric potential obtained from the fluid model with non-local ionization and the simple fluid model are presented and compared.*

Key words: *argon, DC glow discharge, fluid model, non-local ionization*

1. INTRODUCTION

The analysis of gas discharges is very important due to its wide application in different areas of science and technology, e.g. surface sputtering and plasma processing (Lieberman and Lichtenberg, 1994), light sources (Zissis and Kitsinelis, 2009), gas filled switches (Mesyats, 2005; Chang et al., 2011), dielectric barrier discharges (Shkurenkov et al., 2011), welding and thermal processing (Lyndon and Platcow, 2011), etc. For a better understanding of physical processes in different types of gas discharges, a theoretical analysis, i.e. analytical or numerical models must be applied besides experimental investigation. For the modeling of electrical gas discharge there are many different models and all of them can be divided into three groups: fluid, particle and hybrid models (the combination of the first two models). By applying fluid models, the particles of gas are described by equations obtained from the moments of Boltzmann equation. The complete system of equations consists of continuity equations for particles and electron energy balance equation, coupled with Poisson's equations for electric field determination. The first attempt of gas discharge simulation was done by Ward in 1958 (Ward, 1958). He analyzed the effect of space charge in discharge with a cold cathode in

---

Received May 26th, 2015; accepted September 05th, 2015.
[†] Acknowledgement: The authors are grateful to the Ministry of Education, Science and Technological Development of the Republic of Serbia for financial support (Project ON171025).
[*] Contacts of the corresponding author. E-mail: marjansstankov@gmail.com

argon and neon. For the calculation of current density he used an IBM 704 computer. In 1962, he used the same approach for the calculation of potential cathode fall in glow discharge of inert and molecular gases (N_2 and H_2) (Ward, 1962). In 1965, the same author published the paper in which the simulation of electron avalanche in a streamer was performed (Ward, 1965). In this paper, the continuity equation for particles was applied in the form in which it is used today. Following these papers, fluid models have been used very often for the modeling of different types of gas discharges (Lymberopoulos and Economou, 1993; Passchier and Goedheer, 1993; Rafatov et al., 2007; Golubovskii et al., 2003; Rafatov et al, 2012).

In this paper, 2D numerical modeling of DC glow discharge in argon is performed by fluid model with non-local ionization, as well as by simple fluid model for comparison. The modeling is performed for applied voltages $U_w = 300\ V$ and $350\ V$ glow currents $I_g = 110\ \mu A$ and $170\ \mu A$, pressure $p = 1.5\ Torr$ and inter-electrode distance $d = 1\ cm$. The 2D profiles of particle number densities and electric potential obtained from simple fluid model and fluid model with non-local ionization are presented and compared. The paper is organized as follows. A theoretical description of fluid models is given in Section 2. In Section 3, a detailed numerical procedure of 2D numerical modeling is described. Modeling results along with discussion are presented in Section 4, while in Section 5 a short conclusion is given.

2. Simple fluid Model and Fluid Model with Non Local Ionization

The simple fluid model consists of equations obtained from Boltzmann equation (Lieberman and Lichtenberg (1994)):

$$\frac{\partial}{\partial t} f(\mathbf{v},\mathbf{r},t) + \mathbf{v}\cdot\frac{\partial}{\partial r} f(\mathbf{v},\mathbf{r},t) + \mathbf{a}\cdot\frac{\partial}{\partial v} f(\mathbf{v},\mathbf{r},t) = J(f,\mathbf{F}) , \tag{1}$$

where $f(\mathbf{v},\mathbf{r},t)$ is density function, $\mathbf{v}$ is particles velocity, $\mathbf{a} = \mathbf{F}/m$ is particles acceleration and $J(f,\mathbf{F})$ is collision integral. The continuity equation for particles number density, obtained from the zero momentum of Boltzmann equation (1), has the form:

$$\frac{\partial n^{ele,ion}}{\partial t} + \nabla\cdot\mathbf{\Gamma}^{ele,ion} = S \ , \tag{2}$$

where $n^{ele,ion}$ are electron and ion number densities, $\mathbf{\Gamma}^{ele,ion}$ are their flux densities. The source term S includes argon atom ionization by electron impact and electron-ion (Ar^+) recombination:

$$S = \alpha\left|\mathbf{\Gamma}^{ele}\right| - \beta n^{ele} n^{ion} , \tag{3}$$

where α is the first Townsend ionization coefficient and β is electron-ion (Ar^+) recombination coefficient. Fluxes for electrons and ions have the form:

$$\mathbf{\Gamma}^{ele,ion} = \pm\mu^{ele,ion} n^{ele,ion}\mathbf{E} - \nabla(D^{ele,ion} n^{ele,ion}) , \tag{4}$$

where $\mu^{ele,ion}$ are the mobilities of particles and $D^{ele,ion}$ are diffusion coefficients. First term of relation (4) presents the flux of particles due to drift motion, while the second term is diffusion flux. For the calculation of electric potential between the electrodes, Poisson's equation must be included in the model:

$$\nabla^2\varphi = -\frac{e}{\varepsilon_0}(n^{ion} - n^{ele}) , \tag{5}$$

where φ is electric potential, e is elementary charge and ε_0 is vacuum permittivity. The electric field can be calculated from electric potential $\mathbf{E} = -\nabla\varphi$.

The simple fluid model is based on local field approximation, i.e. all transport parameters and rate coefficients are electric field dependent. In gas discharge some of the electrons have enough energy for ionization even in the region of a weak electric field. Because of this, the simple fluid model is not always good enough for the modeling of gas discharges and we must apply the fluid model with non-local ionization. The fluid model with non-local ionization consists of the same equations (2), (5) as the simple fluid model, only the source term is different. This model includes ionization by fast electrons leaving the cathode sheath region, in the glow discharge. The source term for fast electrons has the following form (Rafatov et al., 2012; Stankov et al., 2015):

$$S_{fast}(x) = \begin{cases} \Gamma^{ele}(0)\alpha\exp(\alpha z) & \text{for } z < d_c \\ \Gamma^{ele}(0)\alpha\exp(\alpha d_c)\exp(-(z-d_c)/\lambda) & \text{for } z \geq d_c \end{cases} \tag{6}$$

where $\Gamma^{ele}(0)$ is the electron flux on the cathode, d_c is the cathode sheath region where the electric field is strong, z is the distance from the cathode and λ is the decay constant. The decay constant is calculated from the relation (Rafatov et al., 2012; Stankov et al., 2015; Kudryavtsev et al, 2008):

$$\lambda = \frac{\varphi(d)/(pC-d)}{\alpha d_c} , \tag{7}$$

where $\phi(d)$ is the cathode sheath voltage, while the constant $C = 193\ V/cmTorr$ is calculated from relation (5). Since the external circuit is also included in the modeling, the glow voltage is calculated by substituting the glow current into Ohm's law:

$$U_g = U_w - I_g R , \tag{8}$$

where I_g is glow current, R is resistance, U_w is the working voltage applied to the tube, and U_g is the voltage between electrodes.

3. NUMERICAL PROCEDURE FOR TWO DIMENSIONAL FLUID MODELING

A two-dimensional modeling of DC glow discharge is performed in cylindrical geometry. Because of the axial symmetry of our problem, only the z and r coordinates are taken into account. The fluid equations (2), (5) in cylindrical coordinates have the form:

$$\frac{\partial n^{ele,ion}(r,z,t)}{\partial t} + \frac{1}{r}\frac{\partial}{\partial r}(r\Gamma_r^{ele,ion}(r,t)) + \frac{\partial\Gamma_z^{ele,ion}(z,t)}{\partial z} = S(r,z,t) , \tag{9}$$

$$\frac{1}{r}\frac{\partial}{\partial r}(r\varphi(r,t)) + \frac{\partial^2}{\partial z^2}\varphi(z,t) = -\frac{e}{\varepsilon_0}(n^{ion}(r,z,t) - n^{ele}(r,z,t)) . \tag{10}$$

First, the discretization of space between the electrodes in two dimensions is performed (Fig. 1).

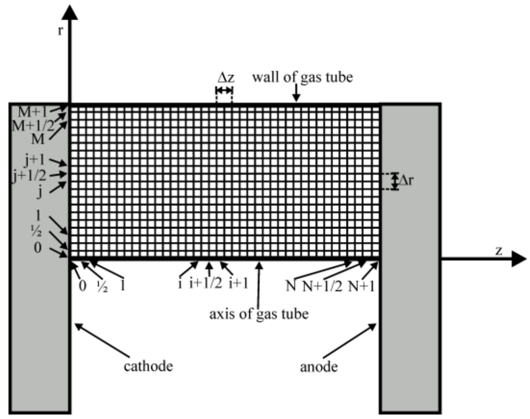

Fig. 1 Discretization of inter-electrode space in two dimensions

The inter-electrode space is divided into $N + 1$ spatial intervals in z direction, where $i = 0$ is the boundary point at the cathode and $i = N + 1$ is the boundary point at the anode. In r direction we made $M + 1$ equal spatial intervals, where $j = 0$ is the boundary point at the axis of the discharge tube and $j = M + 1$ is the boundary point on the tube wall. By applying the finite difference method (Strikwerda, 2004), the relations (9), (10) take the form:

$$\frac{n_{ij}^{ele,\,k+1}-n_{ij}^{ele,\,k}}{\Delta t}+\frac{1}{r_j}\frac{r_{j+1/2}\Gamma_{i\;j+1/2}^{ele,\,k+1}-r_{j-1/2}\Gamma_{i\;j-1/2}^{ele,\,k+1}}{\Delta r}+\frac{\Gamma_{i+1/2\;j}^{ele,\,k+1}-\Gamma_{i-1/2\;j}^{ele,\,k+1}}{\Delta z}=S_{ij} \tag{11}$$

$$\frac{n_{ij}^{ion,\,k+1}-n_{ij}^{ion,\,k}}{\Delta t}+\frac{1}{r_j}\frac{r_{j+1/2}\Gamma_{i\;j+1/2}^{ion,\,k+1}-r_{j-1/2}\Gamma_{i\;j-1/2}^{ion,\,k+1}}{\Delta r}+\frac{\Gamma_{i+1/2\;j}^{ion,\,k+1}-\Gamma_{i-1/2\;j}^{ion,\,k+1}}{\Delta z}=S_{ij} \tag{12}$$

$$\frac{1}{r_j}\frac{\varphi_{i\;j+1}^{k+1}-\varphi_{i\;j}^{k+1}}{\Delta r}+\frac{\varphi_{i\;j+1}^{k+1}-2\varphi_{i\;j}^{k+1}+\varphi_{i\;j-1}^{k+1}}{(\Delta r)^2}+\frac{\varphi_{i+1\,j}^{k+1}-2\varphi_{i\;j}^{k+1}+\varphi_{i-1\,j}^{k+1}}{(\Delta z)^2}=-\frac{e}{\varepsilon_0}(n_{ij}^{ion,\,k}-n_{ij}^{ele,\,k}) \tag{13}$$

After implementation of exponential form for fluxes (Scharfetter and Gummel, 1969), the relations (11), (12) become:

$$A_1^1 n_{i-1\,j}^{ele,\,k+1}+C^1 n_{i\;j}^{ele,\,k+1}+A_2^1 n_{i+1\,j}^{ele,\,k+1}+B_1^1 n_{i\;j-1}^{ele,\,k+1}+B_2^1 n_{i\;j+1}^{ele,\,k+1}=\Delta t\Delta r\Delta z S_{i\;j}^{k}+\Delta t\Delta r n_{i\;j}^{ele,\,k}\,, \tag{14}$$

$$A_1^2 n_{i-1\,j}^{ion,\,k+1}+C^2 n_{i\;j}^{ion,\,k+1}+A_2^2 n_{i+1\,j}^{ion,\,k+1}+B_1^2 n_{i\;j-1}^{ion,\,k+1}+B_2^2 n_{i\;j+1}^{ion,\,k+1}=\Delta t\Delta r\Delta z S_{i\;j}^{k}+\Delta t\Delta r n_{i\;j}^{ion,\,k}\,, \tag{15}$$

where the coefficients A_1^1, C^1, A_2^1, B_1^1, B_2^1, A_1^2, C^2, A_2^2, B_1^2 and B_2^2 are the functions of diffusion coefficients, mobilities and electric potential. After rearranging, Poisson's equation (13) takes the form:

$$A_1^3\varphi_{i-1\,j}^{k+1} + C^3\varphi_{i\,j}^{k+1} + A_2^3\varphi_{i+1\,j}^{k+1} + B_1^3\varphi_{i\,j-1}^{k+1} + B_2^3\varphi_{i\,j+1}^{k+1} = -(\Delta r)^2(\Delta z)^2\frac{e}{\varepsilon_0}(n_{ij}^{ion,\,k} - n_{ij}^{ele,\,k})\,, \quad (16)$$

where coefficients A_1^3, C^3, A_2^3, B_1^3 and B_2^3 are the functions of spatial steps Δz and Δr. Boundary conditions used for the modeling are following: at the cathode ($z = 0$) $\mathbf{\Gamma}^{ele} = -\gamma\,\mathbf{\Gamma}^{ion}$ (γ is the secondary electron yield), $n^{ion} = 0$, $\varphi = 0$; at the anode ($z = d$) $n^{ele,ion} = 0$, $\varphi = U_g$; at the axis ($r = 0$) $\partial n^{ele,ion} / \partial r = 0$, $\partial\varphi/\partial r = 0$ and at the tube walls ($r = R$) $n^{ele,ion} = 0$, $\varphi = U_g\, z / d$.

Matrix representation of linear system of equations for electrons (14) has the form:

$$\begin{bmatrix} C^1 & A_2^1 & 0 & . & 0 & B_2^1 & 0 & . & . & 0 \\ A_1^1 & C^1 & A_2^1 & 0 & . & . & . & . & . & . \\ 0 & A_1^1 & . & . & . & . & . & . & . & . \\ . & 0 & . & . & . & . & . & . & . & 0 \\ 0 & . & . & . & . & . & . & . & . & B_2^1 \\ B_1^1 & . & . & . & . & . & . & . & . & 0 \\ 0 & . & . & . & . & . & . & . & 0 & . \\ . & . & . & . & . & . & . & . & A_2^1 & 0 \\ . & . & . & . & . & . & 0 & A_1^1 & C^1 & A_2^1 \\ 0 & . & . & 0 & B_1^1 & 0 & . & 0 & A_1^1 & C^1 \end{bmatrix} \cdot \begin{bmatrix} n_{11}^{ele,\,k+1} \\ . \\ n_{N1}^{ele,\,k+1} \\ . \\ . \\ . \\ . \\ n_{1M}^{ele,\,k+1} \\ . \\ n_{NM}^{ele,\,k+1} \end{bmatrix} = \begin{bmatrix} \Delta t\Delta r(\Delta z S_{11}^k + n_{11}^{ele,\,k}) \\ . \\ \Delta t\Delta r(\Delta z S_{N1}^k + n_{N1}^{ele,\,k}) \\ . \\ . \\ . \\ . \\ \Delta t\Delta r(\Delta z S_{1M}^k + n_{1M}^{ele,\,k}) \\ . \\ \Delta t\Delta r(\Delta z S_{NM}^k + n_{NM}^{ele,\,k}) \end{bmatrix} . \quad (17)$$

The systems of linear equations for ions and electric potential have the same form in matrix representations as for electrons (17). These linear systems of equations are solved by iterative SOR method (Hoffman, 2001).

The glow current can be determined by integration of the normal component of the current density over the cathode surface. For the calculation of this integral we used the following approximate relation:

$$I_g = e\sum_{j=0}^{m}\pi(r_{j+1} - r_j)^2(|\,\Gamma_{1/2\,j}^{ele}\,| + |\,\Gamma_{1/2\,j}^{ion}\,|)\,, \quad (18)$$

where $\Gamma_{1/2\,j}^{ele,ion}$ are fluxes of particles in the points $i = 1/2$ and $j = 0,...m$ and r_j are distances from tube axis ($r_0 = 0$).

The algorithm of the complete numerical procedure for fluid models is given in Fig. 2. As illustrated in Fig. 2, first we solved the Poisson equation and the values for electric potential are calculated. These values are substituted in the continuity equation for electrons and ions (14), (15) and their number densities are calculated. The procedure is repeated until the difference between the number densities of electrons in two time moments is less than tolerance value a ($|\,n_{ij}^{ele\,k+1} - n_{ij}^{ele\,k}\,| < a$), i.e. until the steady state is reached.

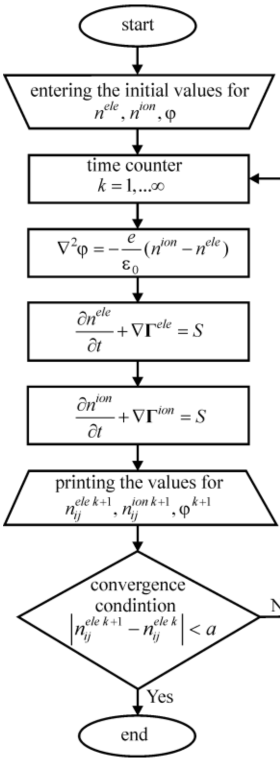

Fig. 2 The algorithm of numerical procedure for fluid modeling

4. Results and Discussion

As said in Introduction, modeling was performed for applied voltages U_w = 300 *V* and 350 *V* and glow currents I_g = 110 *μA* and 170 *μA* at pressure *p* = 1.5 *Torr*. The inter-electrode distance and radius of gas tube are *d* = 1 *cm* and *R* = 1.1 *cm* respectively. The values for mobilities and diffusion coefficients for electrons and Ar^+ ions are taken from (Rafatov et al., 2007; Fiala et al., 1994). The first Townsend ionization coefficient is obtained by fitting the experimental data (Stankov et al., 2015; Kruithof, 1940):

$$\alpha / p = \begin{cases} 0.01\cdot\exp(-\frac{17.77}{E/p}) + 1.24\cdot\exp(-\frac{54.14}{E/p}), & \frac{E}{p} < 15 \\ 4.79\cdot\exp(-\frac{126.93}{E/p}) + 0.88\cdot\exp(-\frac{48.25}{E/p}), & 15 \le \frac{E}{p} < 65 \\ 5.18\cdot\exp(-\frac{102.30}{E/p}) + 10.67\cdot\exp(-\frac{422.01}{E/p}), & \frac{E}{p} \ge 65 \end{cases} . \quad (19)$$

The value of secondary electron yield (γ = 0.02) is obtained from electrical breakdown condition (Stankov et al., 2015). Two dimensional profiles of ion and electron number densities for U_w = 350 *V* and *Ig* = 170 *μA* are presented in Fig. 3.

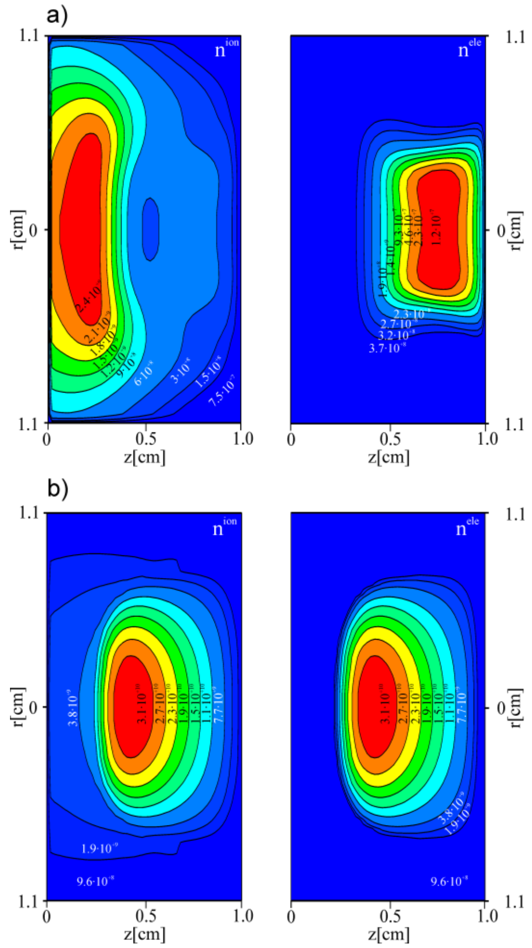

Fig. 3 2D profiles of ion and electron number densities for U_w = 350 *V* and I_g = 170 *μA* obtained from: a) simple fluid model and b) fluid model with non-local ionization

It can be noticed that the values for particle number densities obtained from the fluid model with non-local ionization are higher than those calculated by the simple fluid model, due to the significant contribution of non-local ionization. Also, from 2D profiles it can be seen that the maximum number densities of particles is on the gas tube axis ($r = 0$). The number densities decrease because of particle diffusion towards the tube walls where they recombine. Two-dimensional profiles for $U_w = 300$ *V* and $I_g = 110\mu A$ are not shown because they have a similar form as in the previous case. The number densities of ions and electrons at the axis of the tube for voltages $U_w = 300$ *V* and 350 *V*, glow currents and $I_g = 110\mu A$ and $170\mu A$ are presented in Figure 4.

It is clear that in the case of the simple fluid model, the maximum of ion number densities is close to the cathode, while in the case of the fluid model with non-local ionization the maximum is slightly farther. In both cases the number densities for ions are higher than those for electrons in the region in front of the cathode, which is in agreement with experiment and theory (Raizer, 1991). The difference between ion and electron number densities near the cathode leads to the formation of a cathode sheath region, where the electric field is very strong (Fig. 5). The electric fields obtained from both models have similar axial profiles, except that the cathode sheath length is shorter in the case of the fluid model with non-local ionization.

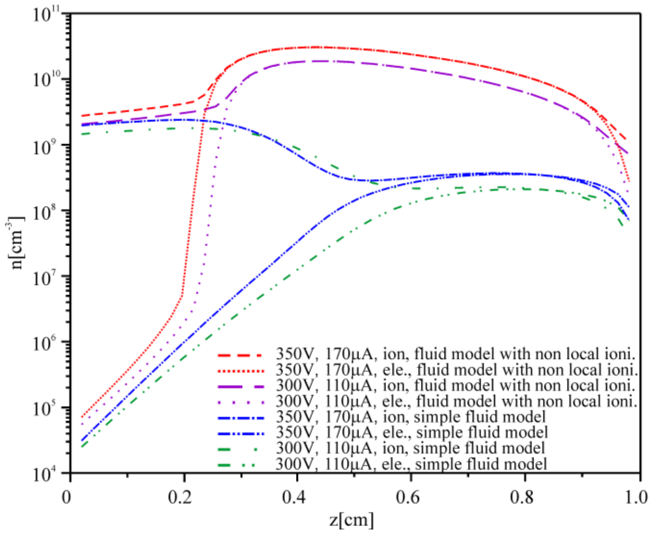

Fig. 4 Particle number densities at the tube axis

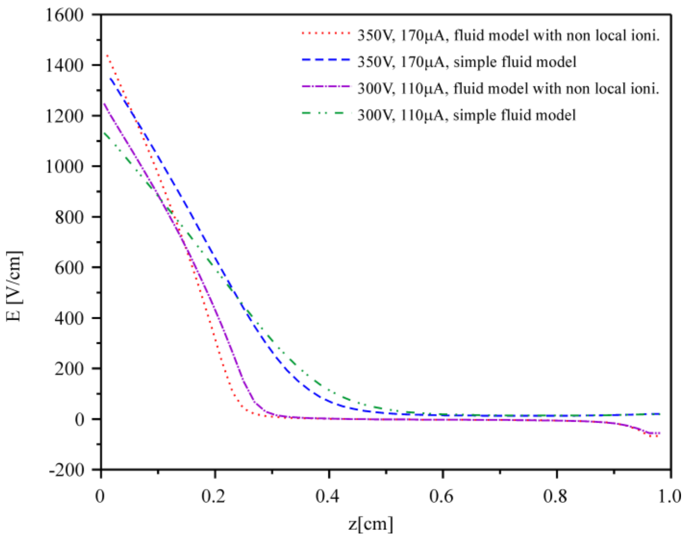

Fig. 5 The electric field at the tube axis

5. CONCLUSION

In this paper, the modeling of DC glow discharge in argon under different conditions of applied voltages and glow currents is performed. The glow discharge is modeled using a 2D fluid model with non-local ionization, as well as a simple fluid model for the sake of comparison. A finite difference method is used for the solving of fluid equations and a detailed numerical procedure for 2D fluid modeling with algorithm is given. The 2D profiles of particle number densities are presented and their values at the axis of the tube are compared. It was noticed that the particle number densities obtained from the fluid model with non-local ionization are higher than those obtained from the simple fluid model, due to the influence of non-local ionization. Similar axial profiles of electric field intensity is obtained from both models, only the cathode sheath length is shorter in the case of the fluid model with non-local ionization. It can be concluded that ionization of fast electrons is not negligible for given conditions and a fluid model with non-local ionization gives more accurate results than a simple fluid model, therefore it is more applicable for gas discharge modeling.

REFERENCES

Chang, J., Wang, H., Zhang, Q., Qiu, A., 2011. Plasma Sci. Technol. 13, 719. doi:10.1088/1009-0630/13/6/16

Fiala, A., Pitchford, L.C., Boeuf, J.P., 1994. Phys. Rev. E, 49, 5607-5622. doi:10.1103/PhysRevE.49.5607

Golubovskii, Y.B., Maiorov, V.A., Behnke, J., Behnke, J.F., 2003. J. Phys. D Appl. Phys., 36, 39-49. doi:10.1088/0022-3727/36/1/306

Hoffman, J.D., 2001. Numerical Methods for Engineers and Scientists, Marcel Dekker, New York.

Jiasen, C., Hu, W., Qiaogen, Z., Aici, Q., 2011. Plasma Sci. Technol., 13, 719-723. doi:10.1088/1009-0630/13/6/16

Kruithof, A.A., 1940. Physica, 7, 519-540. doi:10.1016/S0031-8914(40)90043-X

Kudryavtsev, A.A., Morin, A.V., Tsendin, L.D., 2008. Tech. Phys., 53, 1029-1040. doi: 10.1134/S1063784208080100

Lieberman, M.A., Lichtenberg, A.J., 1994. Principles of Plasma Discharges and Material Processing, John Wiley & Sons, New York.

Lymberopoulos, D.P., Economou, D.J., 1993. J. Appl. Phys., 73, 3668-3679. doi: 10.1063/1.352926

Lyndon, G.S., Platcow, P.A., 2011. Metal Processing and Metal Working Industry, in: Stellman, J.M. (Ed), Encyclopedia of Occupational Health and Safety. International Labour Office, Geneva.

Mesyats, G.A., 2005. Pulsed Power, Springer US, New York.

Passchier, J.D.P., Goedheer, W.J., 1993. J. Appl. Phys., 74, 3744-3751. doi:10.1063/1.354487

Rafatov, I.R., Akbar, D., Bilikmen, S., 2007. Phys. Lett. A, 367, 114-119. doi:10.1016/j.physleta.2007.02.073

Rafatov, I., Bogdanov, E.A., Kudryavtsev, A.A., 2012. Phys. Plasmas, 19, 093503(1)-0093503(8). doi:10.1063/1.4752419

Raizer, Y.P., 1991. Gas Discharge Physics, Springer, Berlin.

Scharfetter, D.L., Gummel, H.K., 1969. IEEE T. Electron. Dev., 16, 64-77. doi:10.1109/T-ED.1969.16566

Shkurenkov, I.A., Mankelevich, Y.A., Rakhimova, T.V., 2011. Eur. Phys. J. D, 62, 213-218. doi: 10.1140/epjd/e2011-10653-y

Stankov, M.N., Petković, M.D., Marković, V.Lj., Stamenković S.N., Jovanović, A.P., 2015. Chinese Phys. Lett., 32, 025101(1)-025101(5). doi:10.1088/0256-307X/32/2/025101

Strikwerda, J.C., 2004. Finite Difference Schemes and Partial Differential Equations, Society for Industrial and Applied Mathematics, Philadelphia.

Ward, A.L., 1958. Phys. Rev., 112, 1852-1857. doi:10.1103/PhysRev.112.1852

Ward, A.L., 1962 J. Appl. Phys., 33, 2789-2794. doi:10.1063/1.1702550

Ward, A.L., 1965. Phys. Rev., 138, 1357-1362. doi:10.1103/PhysRev.138.A1357

Zissis, G., Kitsinelis S., 2009. J. Phys. D Appl. Phys. 42, 173001-17500. doi:10.1088/0022-3727/42/17/173001

DVODIMENZIONALNI FLUIDNI MODEL JEDNOSMERNOG TINJAVOG PRAŽNJENJA U ARGONU NA NISKOM PRITISKU

U radu je izvršeno modelovanje jednosmernog tinjavog pražnjenja u argonu na pritisku p = 1,5 Torr i međuelektrodnom rastojanju d = 1 cm pri različitim vrednostima primenjenih napona i radnih struja tinjavog pražnjenja. Po prvi put je modelovano tinjavo pražnjenje u argonu dvodimenzionalnim fluidnim modelom sa nelokalnom jonizacijom. U radu je data detaljna procedura za 2D fluidni model. Osim toga, izračunate su i upoređene 2D raspodele koncentracija čestica i električnog potencijala dobijenih pomoću fluidnog modela sa nelokalnom jonizacijom i jednostavnog fluidnog modela.

Ključne reči: *argon, jednosmerno tinjavo pražnjenje, fluidni model, nelokalna jonizacija*